Rainfall Intensity (RI)
Algorithm Theoretical Basis Document

(RI-v1.0)

NMSC/SCI/ATBD/RI, Issue 1, rev.0

2012.12.12

National Meteorology Satellite Center

REPORT SIGNATURE TABLE

Function	Name	Signature	Date
Prepared by			
Reviewed by			
Authorised by			

DOCUMENT CHANGE RECORD

Version	Date	Pages	Changes

Table of Contents

List of Tables

List of Figures

List of Acronyms

ACC	Accuracy
AWS	Automatic Weather Station
ARKT	Arkin Technique
BTT	Brightness Temperature
CDF	Cumulative Distribution Function
CMDPS	COMS Meteorological Data Processing System
CMORPH	CPC MORPHed precipitation
COMS	Communication, Ocean, and Meteorological Satellite
CST	Convective-Stratiform Technique
DPM	Data Processing Module
DMSP	Defense Meteorological Satellites Program
FTP	File Transfer Protocol
GMSRA	GOES Multispectral precipitation Algorithm
GPI	Goes Precipitation Index
HSS	Heidke Skill Score
LUT	Look-Up Table
MTSAT-1R	Multi-functional Transport Satellite
NAWT	Negri-Adler-Wetzel Technique
NOAA	National Oceanic and Atmospheric Administration
PC	Proportion Correct
PDF	Probability Distribution Function
POD	Probability of Detection
POM	Post-Processing Module
PMM	Probability Matching Method
QC	Quality Control
RMSE	Root Mean Square Error
SCaMPR	Self-Calibrating Multivariate Precipitation Retrieval
SSM/I	Special Sensor for Microwave Imager
TS	Threat Score
UTC	Coordinated Universal Time
VAM	Validation Module

1. Overview

Rainfall intensity calculation by CMDPS is an empirical estimation using infrared channel brightness temperature of COMS and rainfall intensity data of SSM/I. In an indirect RI calculation like this, a certain degree of error caused by change of relationship between two satellite data is inevitable. However, it can be very useful in real time forecast of severe rain storm following adverse weather, since it is easy to calculate the hourly change of rainfall across a wide area. To calculate temporal and spatial distribution of rainfall in Eastern Asian region, rainfall intensity calculation Look-Up Table(LUT)of land and ocean for microwave data for 36 hours prior to COMS observation was used real time, and stable rainfall intensity was maintained by applying a static LUT with the average for a certain period. The result of RI is compared and verified with automatic weather observation system (AWS) data in Korean peninsular area and the measurement by SSMI/I satellite in Eastern Asia.

Historical background of CMDPS RI calculation will be discussed in Chapter 2. In Chapter 3, theoretical background, calculation and evaluation methodology will be described. In Chapter 4 and 5, interpretation of calculation result, problems and areas of improvement of RI algorithm will be discussed.

2. Background and Purpose

Infrared and visible observation data from COMS provide temporal and spatial information useful to calculate RI such as the brightness temperature, radiative emission and reflectivity of cloud produced by mesoscale system change. Normal method to estimate RI by geostationary satellite is to use empirical relation between satellite brightness temperature data and RI observed on the ground. However, the spatial distribution of ground RI by direct observation is limited, and temporal and spatial mismatch with satellite observation data makes it hard to perform an accurate empirical calculation. RI changes differently depending on type, developmental status of cloud and area and time, and this makes RI calculation even harder.

In the result of research, Levizzani(1999) suggested that the rainfall observed on the ground was related to the characteristics of top part of cloud and rainfall can be estimated using infrared channel of a geostationary satellite. Inaccuracy of microwave algorithm can increase as the altitude of satellite orbit becomes higher, however, various RI estimation methods based on microwave theory were developed using data from SSM/I (Special Sensor Microwave/Imager, Wentz and Spencer, 1998; Spencer et al., 1989). Recently, a mixed method of microwave and infrared channel of geostationary satellite is used in numerical model data assimilation and real time operation research. Microwave and radar data are used in various ways to supplement RI data observed on the ground (Turk et al., 2003; Weng et al., 2003; Vincente et al., 1998).

RI estimation methods only with infrared channel of geostationary satellites include studies such as LUT(Kurino,1997), CST(Convective-Stratiform Technique; Adler and Negri, 1988), NAWT(Negri et al., 1984) and ARKT(Arkin, 1979), however, precipitation time and regional change property were not properly analyzed because no algorithm specific to certain time and region was reflected. Studies in which RI was indirectly estimated using cloud elements observed and calculated by geostationary satellites such as cloud top temperature, cloud optical thickness, cloud height, cloud amount and shape include GPI(Goes Precipitation Index; Arkin and Meisner, 1987), Autoestimator(Vincente, 2002), Hydroestimator(Scofield and Kuligowski, 2003), GMSRA(Ba and Gruber, 2001), but the algorithm used in these studies implies problems of temporal and spatial limit. Studies that mixed visible light/infrared data and microwave data included CMORPH(Joyce et al., 2004), SCaMPR(Kuligowski, 2002), and GPROF(Kummerow et al., 2001). These methods have relatively high accuracy compared to the methods suggested above, but method of satellite observation and temporal and spatial discordance are pointed out as problem. Recently, a rainfall estimation method using cloud categorization and lifetime of mesoscale convective system (Delgado et al., 2008) and methods using artificial neural network (Sorooshian et al., 2000; Zhang and Scofeld, 1994) have been introduced, however, analysis of related elements and rapid changes occurring real time are not being reflected properly.

CMDPS RI is based on the relation between brightness temperature data of geostationary satellite and SSM/I rainfall data, and it is empirically calculated by applying PMM(Probability Matching Method) by Atlas et al.(1990) and Crosson et al.(1996). In this case, as SSM/I rainfall data has different algorithm applied between land and sea, COMS brightness temperature data was calculated differently for land and sea. Because of the temporal discrepancy following the delay of SSM/I observation time, data collection and transmission time, a method to make temporal and spatial coincidence between SSM/I data for 36 hours before CMDPS measurement time and CMDPS data (dynamic LUT) was used. However, when SSM/I data is delayed more than for 36 hours or in an emergency situation with absence of data, average data for a certain period (static LUT) is used. SSM/I data is used to evaluate the product of the resulted RI calculation in Eastern Asian region, and AWS rainfall data is used for Korean peninsular.

In RI calculation by CMDPS, some improvement of accuracy is expected if calculation area and cloud type are limited. But, high accuracy is not expected due to basic channel limitation. Nevertheless, as RI calculation by geostationary satellite is carried out 48 times a day every 30 minutes for north hemisphere, it can be used as an important data to predict the real time RI and temporal and spatial change of RI. And it can largely contribute to improve forecasting ability when it is used as numerical model input data, because of the temporal continuity and spatial density property.

3. Algorithm

3.1. Theoretical Background

10.8 and 12㎛ sensors mounted on a geostationary satellite react sensitively to water vapor in the atmosphere, and it provides cloud top temperature and cloud height if there is any cloud. High cloud height means low cloud top temperature and ground rainfall in the cloud area like this is shown to be high (Arkin and Meisner, 1987, Adler and Negri, 1988). Different from geostationary satellite method, RI calculation by microwave satellite is done by a direct method with radiative emission and scattering property by cloud particle of water droplet or ice (Wentz and Spencer, 1998; Spencer et al., 1989). CMDPS uses the continuous observation characteristics of geostationary satellite like above and accurate precipitation data by SSMI, and the relation between them can be shown like follows. Accurate temporal and spatial coincidence of two satellites plays an important role.

$$ {}^{R_i} \quad R)dR = \int_{BTT_t}^{BTT_i} P(BTT)dBTT \qquad (1) $$

Equation (1) indicates the relationship between brightness temperature of a geostationary satellite (COMS) and SSM/I data. It is PMM(Probability Matching

Method) suggested by Atlas et al.(1990) and Crosson et al.(1996) and R is the rainfall of SSM/I and BTT is the brightness temperature of COMS infrared channel. This equation calculates the value of BTT_i and R_i when CDFs (Cumulative Distribution Functions) of BTT and R match, assuming that the probability distribution function of BTT of COMS infrared channel and the probability distribution function of SSM/I rainfall R are similar.

3.2. Methodology

RI calculation methodology by satellite data can be divided into brightness temperature (T11) of geostationary satellite, temporal and spatial coincidence data creation process of SSM/I data, and calculation of PMM and look up table for land and sea pixel. SSM/I(Wentz and Spencer, 1998; Spencer et al., 1989) is a microwave sensor mounted on DMSP F13~F15 for the purpose of rainfall measurement, with resolution of 25km×25km. SSM/I sensor observes Eastern Asian area (90˚E~160˚E, 10˚N~60˚N) for more than 20 times a day, but temporal and spatial discrepancy occurs with geostationary satellite as seen in Figure 1. shows the observation time of Eastern Asian region by microwave satellite such as SSM/I on July 14, 2007.

As seen in this figure, F13~F15 are SSM/I data and its single observations about 120 minutes and up (black solid line). Red (ascending node) and green (descending node) rectangles are observations time of Eastern Asian region. Eastern Asian region is observed for 23 times a day. However, recently, observation of F13 and F14 were terminated (F13:November 2009, F14:August 2008), so the number of observation of Eastern Asia for a day was rapidly reduced to 8 times a day. Using the information of Figure 1, SSM/I and geostationary satellite pixel were time coincided and brightness temperatures of geostationary satellites within the observative resolution (12.5km) of SSM/I were averaged to make spatial coincidence. In the case of microwave satellite, rainfall is calculated by different algorithms for sea and land pixel, so temporal and spatial coincident data was made separately for land and sea. Figure 2 is the temporal and spatial coincidence result of satellite brightness temperature of land, sea, and total (land + sea), and SSM/I precipitation at 0745UTC April 27, 2011.

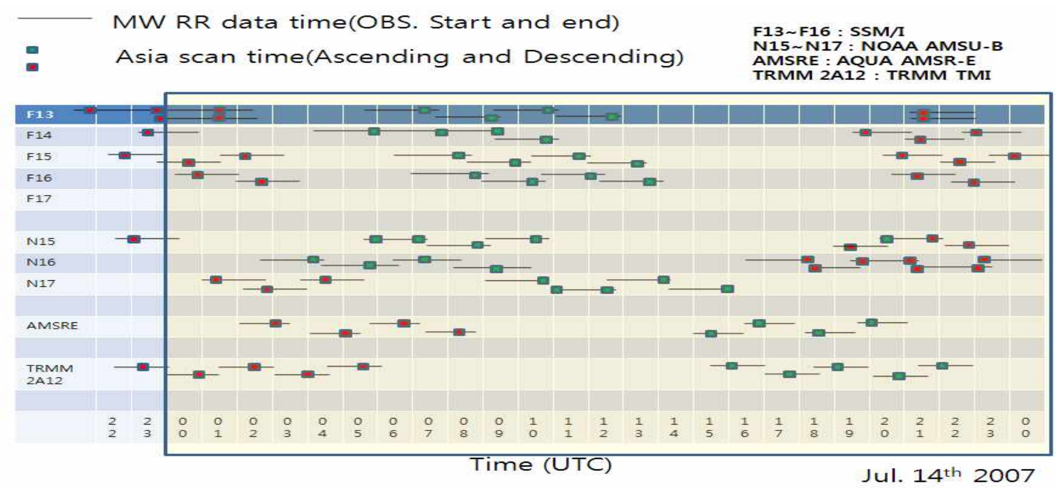

Figure 1. Microwave data for east asia region at July 14 2007.

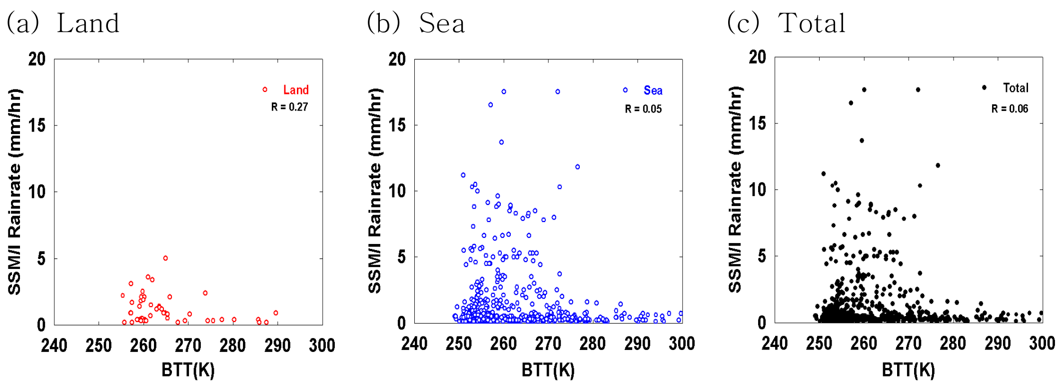

Figure 2. Temporal and spatial coincident between COMS BTT and SSM/I rainrate at 0745UTC April 27 2011.

As seen in this figure, correlation between satellite brightness temperature and SSM/I precipitation was higher in land pixel than sea.

As seen in Figure 1, because of SSM/I observation time, data processing and transmission time for Eastern Asian area by F15, up to 16 hour gap can occur per day in SSM/I rainfall data. Therefore, in the result of analysis on the number of temporal and spatial coincidence data of Eastern Asian region from April 15 to 17, 2007, it was found that there was no coincidence data from April 15, 0000~0700UTC and 1500~2400UTC, as seen in Figure 3.

To resolve this data blank, real time look up table was made using the data 36 hours before COMS observation time as temporal and spatial coincidence data. When the number of dynamic look up table is low (less than 30), static look up table was used. In this case, PPM suggested by Atlas et al.(1990)and Crosson et al.(1996) was used for COMS brightness temperature and SSM/I rainfall data. Minimum SSM/I rainfall is defined as 0.5mm/hr. Figure 4 shows brightness temperature and PDF and CDF of SS M/I precipitation applied at 0745UTC April 27 2011.

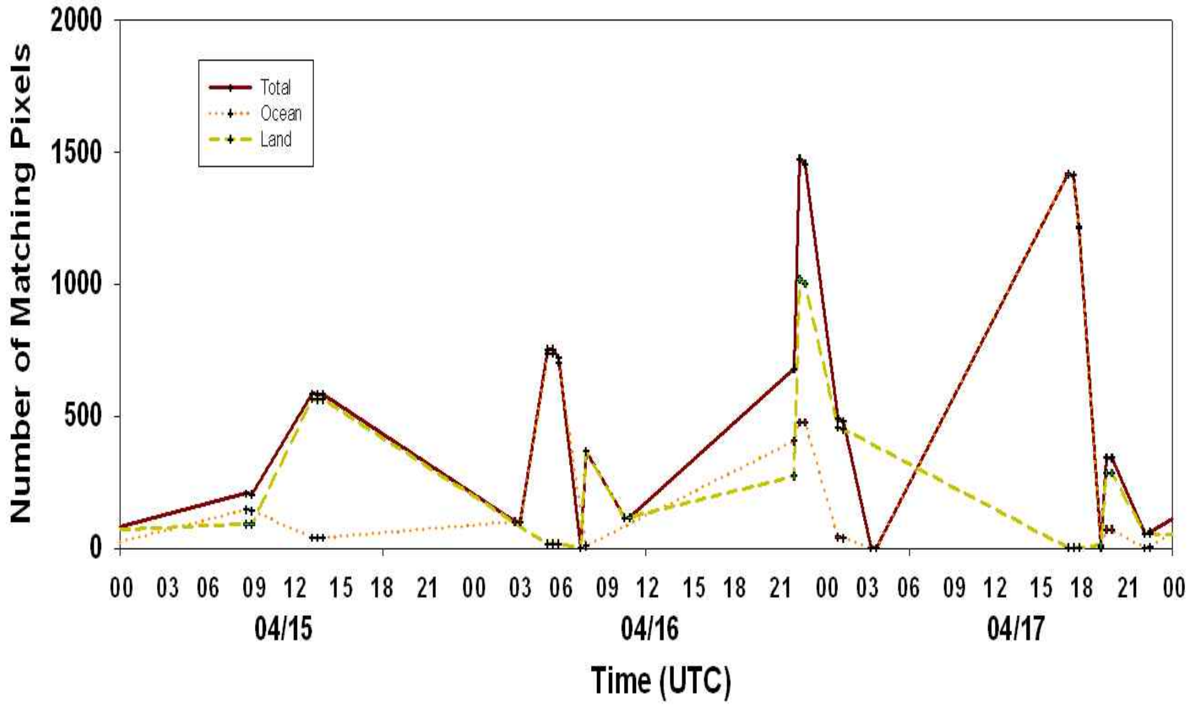

Figure 3. Temporal and spatial coincident data between COMS BTT(brightness temperature) and SSM/I (F15) rainrate from 0033UTC April 15 2011 to 2333UTC April 17 2011.

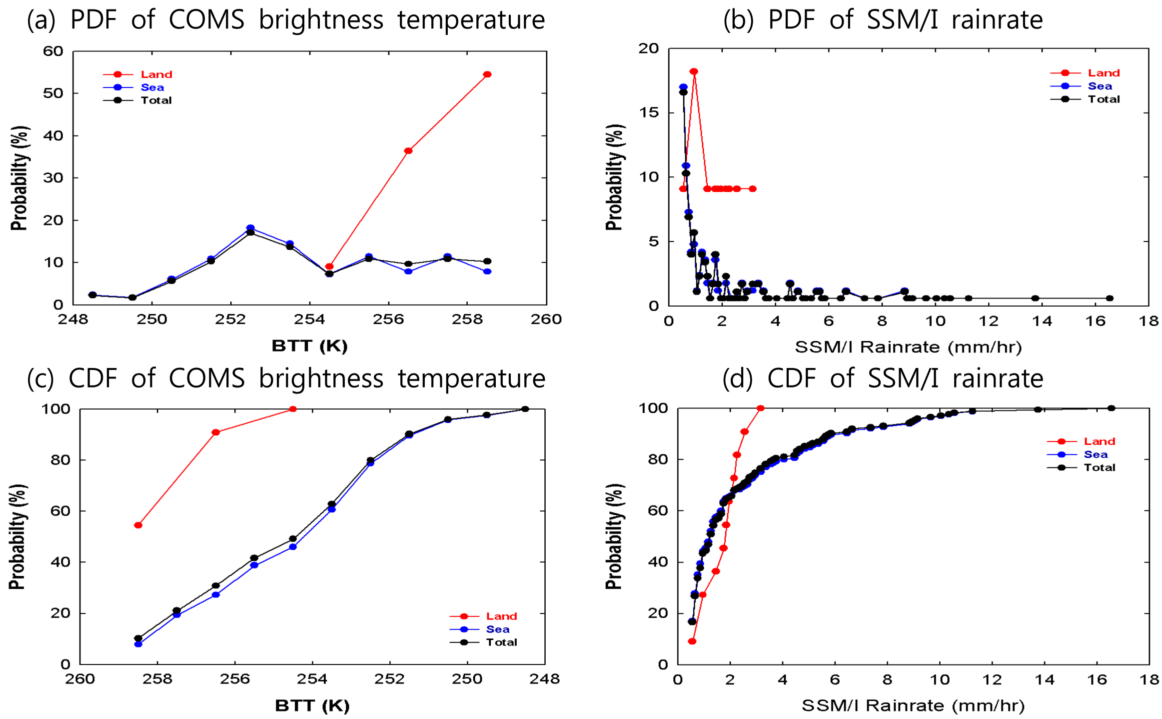

Figure 4. PDF and CDF of COMS BTT(Brightness temperature) and SSM/I rainrate at 0745UTC April 27 2011.

The look up table calculated at 0745UTC April 27 2001 using brightness temperature and rainfall that show the same cumulative probability in (c) and (d) of Figure 4 are shown in Figure 5.

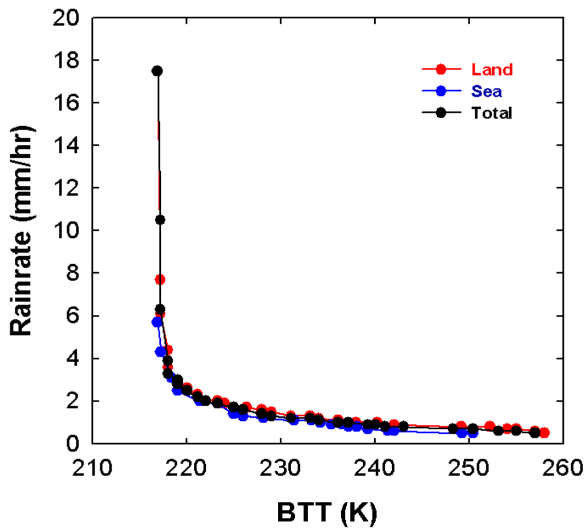

Figure 5. Lookup table between COMS BTT(brightness temperature) and SSM/I rainrate at 0745UTC April 27 2011.

The look up table calculated as Figure 5 calculates rainfall by making a look up table for land and sea, separately. However, as shown in Figure 6, the number of look up table for land area is remarkably smaller than the number of look up table for sea area. Figure 6 shows the number of look up table calculated for the whole area of land and sea in April 2011. This lack of look up table on the land area causes spatial discontinuity between land and sea on rainfall area. That is, a spatial discontinuity between land and sea is shown as (a), RI at 0400UTC July 10 2011. Therefore, when LUT of land area is made, a continuous precipitation pattern like (b) of Figure 7 can be calculated if the RI is estimated using the point match result of total area (land + sea) by adding the data on the sea area. RI for the brightness temperature not found on LUT is calculated by linear interpolation, and the calculated rainfall was adjusted to latitude to resolve over-simulation at high latitude. The maximum RI calculated here cannot exceed 35 mm/hr and the minimum was limited to 0.5mm/hr. In the case of cirrus, of which cloud brightness temperature is low but which is relatively thin, infrared temperature difference (Inoue, 1987; 2002) was applied and it was separated as non fainfall area when the temperature difference is 2.5K and up.

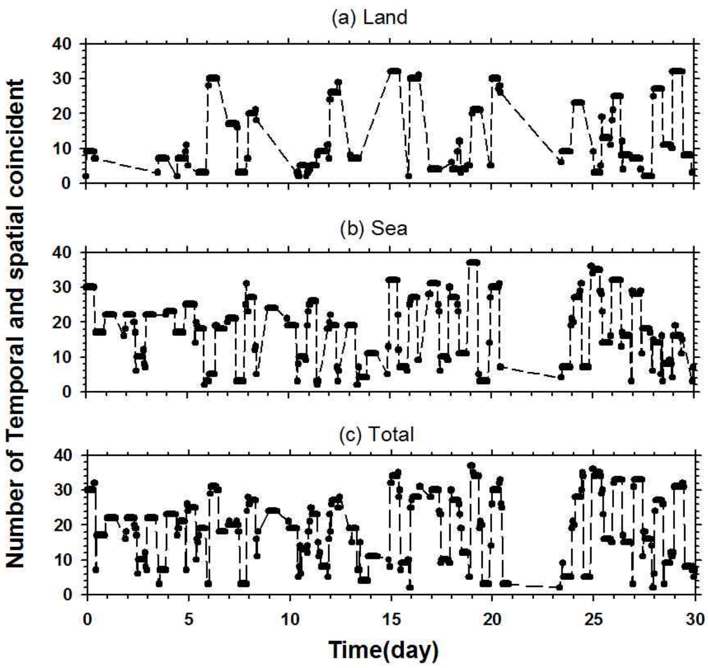

Figure 6. Time series for Number of data pairs in estimated LUTs in April 2011.

(a) Before (b) After

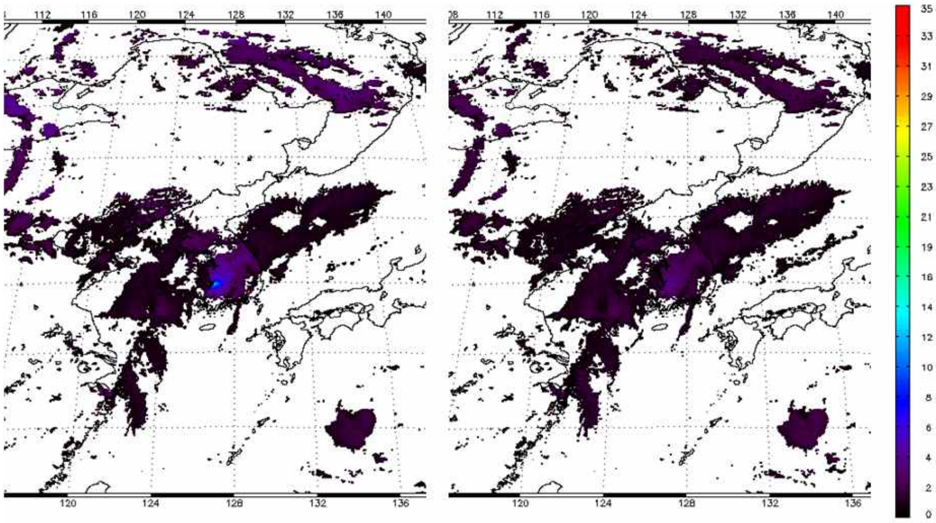

Figure 7. Estimated precipitation intensity images at 0400UTC July 10 2011.

3.3. Calculation Process

In RI calculation by CMDPS, LUT preparation using COMS and SSM/I data, RI calculation using the result, and test and quality control process are important, and it is roughly divided into RI calculation (DPM) and post-treatment (POM) processes. In DPM process, rainfall is calculated by using calculation data and LUT calculated from post-treatment, and in POM process, LUT of RI calculation is calculated using COMS channel data and SSM/I rainfall data. When there is sufficient amount of temporal coincidence data of COMS and SSM/I data due to the delay of observation, data collection and transmission of SSM/I, RI may not be calculated. Therefore, SSM/I data for 36 hours before COMS observation is used to calculate LUT and this process can be diagrammed as CMDPS RI calculation algorithm in Figure 8.

3.3.1 Input Data

For input data to calculate CMDPS RI, infrared channel brightness temperature and geolocation by pixel, and land and sea masking data are essential from COMS 1.5b channel data. CMDPS cloud detection(CLD) result, quality information and SSM/I data are used as auxiliary data to calculate RI. 15 minute accumulated rainfall by AWS in

Korean peninsular and SSM/I rainfall data are used for evaluation data.

COMS 1.5b data is a brightness temperature converted into temperature value from data observed by geostationary satellite sensor by radiation test. It contains latitude and longitude information of each pixel. Among CMDPS RI calculation elements, cloud detection data is used to make with/without rainfall calculation. SSM/I is an important input data to calculate RI interaction formular in relation to COMS infrared channel brightness temperature change. If any error is included in SSM/I data, it directly affects the quality of CMDPS calculated. Auxiliary data used in rainfall calculation must be renewed real time by FTP, and data renewal is required to be confirmed by driving data extraction program. Each auxiliary data is distributed to RI calculation, temporal and spatial data creation/evaluation and post treatment by extraction program provided during the observation data creation process.

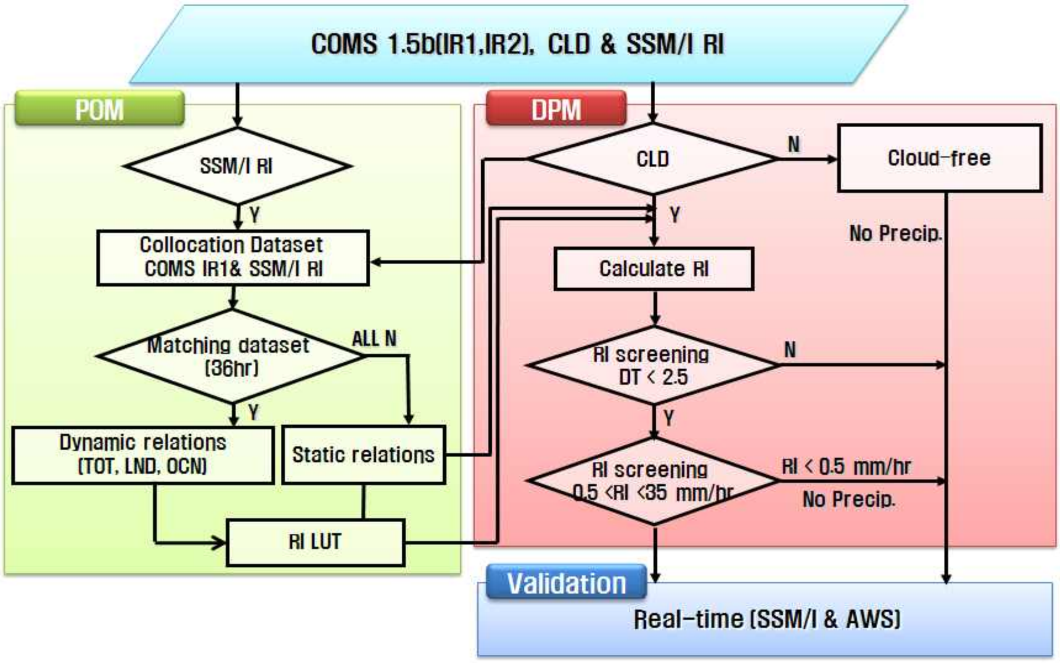

Figure 8. Flow chart for the CMDPS RI algorithm.

3.3.2 DPM Process

DPM process to calculate RI following channel data observed from COMS satellite, cloud detection data, and LUT created from post-treatment can be shown as Figure 9.

Figure 9. The Schematic diagram for the RI DPM procedure.

As RI is calculated for cloud pixel, cloud and clear pixel should be first distinguished using cloud detection result. Each cloud pixel is classified into land or sea pixel, and RI is calculated according to RI LUT obtained from POM process. However, as the minimum cloud top temperature and maximum rainfall are now always found during the LUT preparation, discontinuity takes place in RI over time. Therefore, RI calculation scope is extended by interpolation with the LUT calculated considering the lowest cloud top temperature (190K) and maximum RI (35mm/h). Figure 10 shows the time series of existing LUT and LUT calculated by applying minimum cloud top temperature and maximum RI.

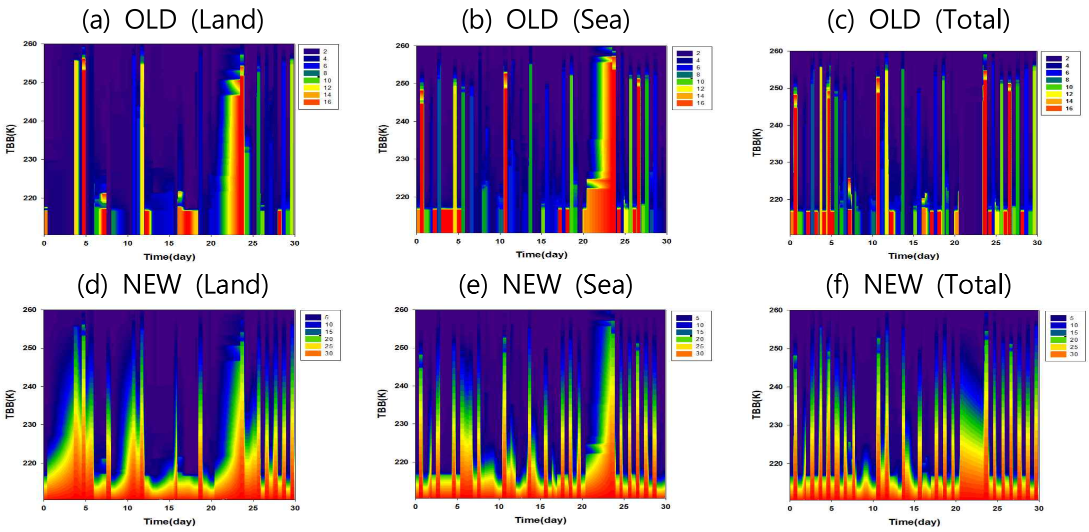

Figure 10. The time series of LUTs for the CMDPS RI algorithm.

To resolve over estimation of rainfall at high latitude, latitude was adjusted by using following empirical formular for the calculated precipitation.

$$I \quad RI\,(1.8545-0.0934\,lat-0.0028lat^2-2.733-5\times lat^3) \qquad (2)$$

$$RI = RI_1\,(1.670-0.0819\,lat-0.0026lat^2-2.874-5\times lat^3) \qquad (3)$$

Here, at is latitude, I is rainfall calculated by applying LUT, and RI is the rainfall with adjusted latitude. The equation (2) was calculated using point match data between COMS cloud brightness temperature created to make land LUT and SSM/I rainfall, and the equation (3) was calculated using point match data between COMS cloud brightness temperature created to make sea LUT and SSM/I rainfall. It is the empirical formular calculated by classifying the relation between cloud top temperature and RI by latitude band, and applying latitude function to the ratio of rainfall at each latitude band to the rainfall at a specific latitude (10°N).

For the calculated rainfall, cloud optical thickness in rainfall area and RI range test were performed. To remove thin cloud pixel without precipitation, pixels with temperature difference more than 1.2K are removed as non rainfall pixel, and minimum using infrared temperature difference method (Inoue,1987;2002)and maximum Ri were set to 0.5 and 35 mm/hr to remove under- and over-calculated pixels. On the final stage, RI calculation process and quality control information on pixel characteristics are prepared. Figure 11 is an example of calculated RI quality test information for global area at 0033UTC November, 7, 2008.

(a) Estimated RI (b) Quality flag

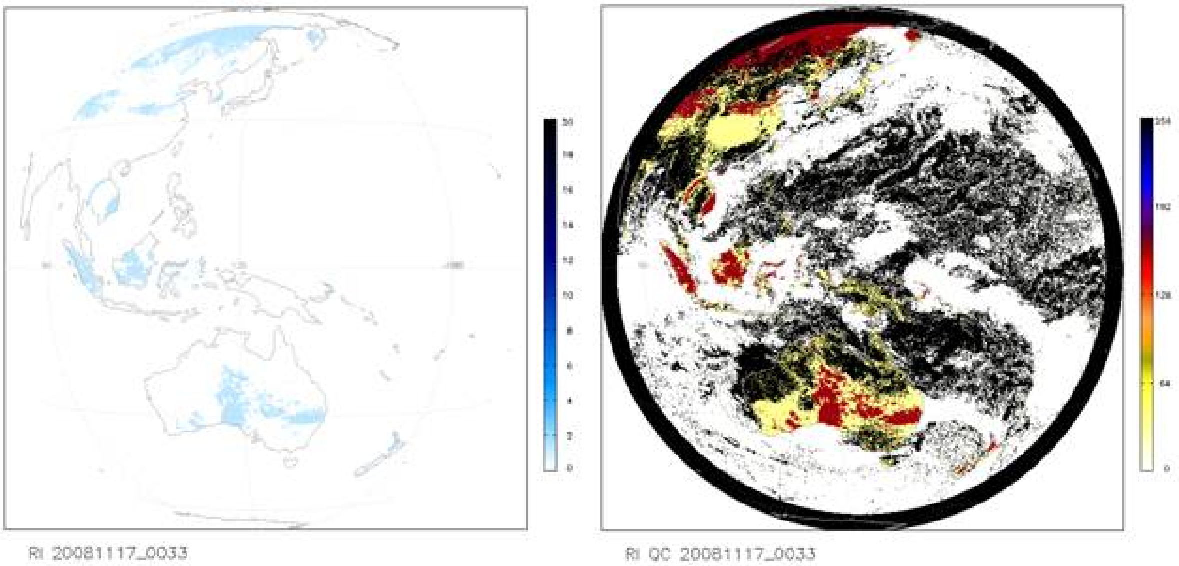

Figure 11. Estimated CMDPS RI and quality flag image on 0033UTC November 17. 2008.

QC(Quality control) of calculated RI data are for cloud pixel screening data, information on land and sea, information on infrared difference method, and rainfall calculation information as seen in Table 1. Quality information of RI result is calculated for each pixel and calculation is expressed as value from 1 to 256.

Table 1. Quality flag for the CMDPS rainfall intensity.

Parameter	Value	Meaning
Quality flag	256	Not significant
	1	Cloud product quality information : Cloud pixel (100%)
	2	Cloud product quality information : Cloud pixel (75%)
	3	Cloud product quality information : Cloud pixel (50%)
	4	Cloud product quality information : Clear sky pixel (75%)
	5	Cloud product quality information : Cear sky pixel(100%)
	16	Precipitation removal pixel by infrared temperature difference
	32	Land and coast pixel
	64	Clear sky pixel
	128	Precipitation calculation pixel

3.3.3 POM Process

POM process is a RI relation formular calculation stage and it is largely divided into two parts. It is a stage of land and sea LUT preparation using COMS brightness temperature, temporal and spatial coincidence of SSM/I rainfall , and temporal and spatial coincidence data for 36 hours before COMS observation. Temporal coincidence between geostationary satellite (COMS) and microwave satellite (polar orbit satellite) with different observation characteristics is carried out to each pixel using time information per observation pixel of COMS data and time information per pixel of SSM/I. For spatial coincidence, land and sea classification is done first for each COMS data pixel, and spatial coincidence was carried out by averaging the pixels of COMS included in the spatial resolution (25 Km × 25 km) of SSM/I. On LUT preparation stage, PMM method is applied by searching temporal and spatial coincidence data within 36 hours before COMS observation time. LUT was calculated for land and sea with up to 41 pairs of brightness temperature and rainfall by dividing time/space coincided SSM/I rainfall and cumulative probability distribution of COMS brightness temperature by 2.5 %. Due to the characteristics of SSM/I data, the reliability of calculation result can be largely reduced if the number of temporal and spatial coincidence data is too low. This POM process is shown in Figure 12. In this picture, green rectangle part (POM_Coll) is temporal and spatial coincidence stage and blue rectangle part (POM_Coeff) is LUT preparation stage. Temporal and spatial coincidence data was averaged for a long term (10 days or more) to prepare semi-real time LUT, and when temporal and spatial coincidence data lacks, (less than 30 dynamic LUT), static LUT is used to calculate RI.

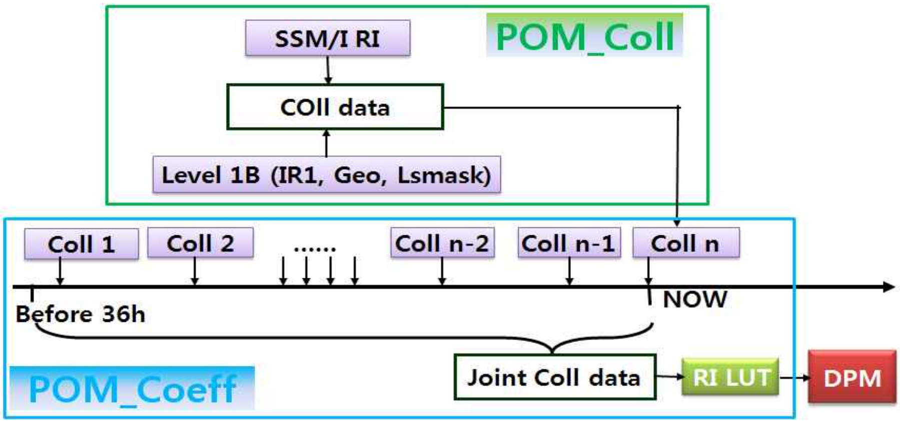

Figure 12. Diagram for the CMDPS RI POM procedure.

3.4. Evaluation

3.4.1. Evaluation Methodology

Evaluation of RI result is carried out using ground AWS rainfall data of Korean peninsular and SSM/I RI data in Eastern Asian area. As these data are renewed through network, it is evaluated semi-real time, not real time. Evaluation of RI calculation result and observation data is divided into two parts of temporal and spatial coincidence process and evaluating calculation as in Figure 13 due to the observation method and temporal and spatial discrepancy between data.

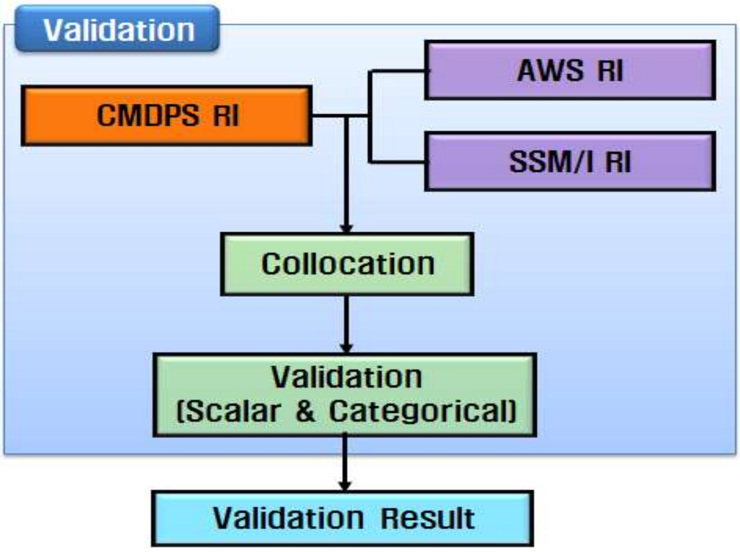

Figure 13. Flow chart for the validation of CMDPS rainfall intensity.

To make temporal and spatial coincidence, time is coincided with CMDPS RI considering the data characteristics of AWS observation and SSM/I RI and space is coincided with resolution and range of application. In particular, temporal and spatial coincidence of SSM/I RI is same as that of POM process, and evaluation is done with scalar accuracy test by rainfall and categorical accuracy test by presence and intensity of rainfall. For scalar accuracy test, correlation coefficient, bias, and root mean square error (RMSE) are used and for categorical accuracy test, it is analyzed into TS(Threat Score), POD(Probability of Detection), PC(Portion Correct) and HSS(Heidke Skill Scores) by applying multiple categorization method of mild, intermediate, and strong for 3, 5, and 10mm/hr according to RI and dual categorization method of with/without rainfall.

3.4.2. Evaluation Material

To evaluate COMS RI result, AWS rainfall observation data of about 600 points of Korean peninsular and SSM/I RI data of Eastern Asia (90~160˚E, 10~60˚N) are used.

A. Korean peninsular

AWS rainfall, 15 minutes accumulated data on manned/unmanned observation stations (about 600) in Korean peninsular is used. The interval of data observation is 1 minute and unit of rainfall is 0.1 or 0.2 mm, and the data is accumulated for of every 15 minutes or for every 60 minutes. As CMDPS calculated RI is the momentary observation result by a geostationary satellite (COMS), rainfall accumulated for 15 minutes is used for ground observation data, considering the time affecting the cloud and rainfall observation. Considering AWS distribution in Korean peninsular, observation area is averaged for surrounding 30 km×30 km and time and space are coincided with CMDPS calculated RI.

B. Eastern Asian area

SSM/I RI is data from sensor of polar orbit satellite, and it is mounted on 1 satellite of F15 playload and calculated based on the emission and scattering radiation of raindrop and ice crystal in cloud. One polar orbit satellite observes one same point 2 times a day, and the resolution of the sensor is 25 km × 25 km at sub-satellite point. It is evaluated by using data from Eastern Asia (90~160˚E, 10~60˚N) and time and space are coincided in the same method as POM process.

3.4.3. Temporal and Spatial Coincidence

AWS and SSM/I data used in CMDPS RI result evaluation have different observation method and period, so careful temporal and spatial coincidence process is required to evaluate CMDPS RI result. AWS accumulated rainfall data is coincided in time with the observation data for 20 minutes after COMS observation time, considering the falling time of rainfall particle and 15 minutes accumulation characteristics. Observation is made on about 600 points in Korean peninsular and the observatory radius of one AWS point is 30 km×30 km. CMDPS calculated rainfall in 7×7 pixel included in each observatory radius is averaged to make spatial coincidence.

For SSM/I RI data, time of each pixel and time of each COMS pixel are calculated and delayed by 15 minutes to make temporal coincidence. CMDPS RI data with 12.5km radius based on the SSM/I sub-satellite point (25 km × 25 km)is averaged to make spatial coincidence.

3.4.4. Evaluation Result Analysis

To evaluate CMDPS RI calculation result, rainfall area detection and evaluation of rainfall intensity are important elements as well as accuracy determination by comparing with observation data. Scalar accuracy test and categorical accuracy test are performed as evaluation. To make a scalar accuracy test, correlation coefficient, bias, and root mean square error(RMSE) are calculated. To make a categorical accuracy test, the accuracy to determine the presence of rainfall is evaluated based on 0.5 mm/hr. For multiple categorical accuracy test, the accuracy of rainfall intensity determination for rainfall data is calculated as POD(Probability of Detection), PC(Portion Correct) and HSS(Heidke Skill Scores) based on 3, 5, 10 mm/hr.

A. Scalar accuracy test

Scalar accuracy test is to test the accuracy of quantity of rainfall. Correlation coefficient between observation and calculated rainfall, bias that indicates the bias of result toward average value, and SMSE to evaluate the standard error of the result are calculated like follows:

Correlation coefficient
$$\frac{\frac{1}{n}\sum_{i=1}^{n}(x_i-\overline{x_i})(\hat{x_i}-\overline{\hat{x_i}})}{\frac{1}{n}\sum_{i=1}^{n}(x_i-x_i)^2\sqrt{\frac{1}{n}\sum_{i=1}^{n}(\hat{x_i}-\overline{\hat{x_i}})^2}} \quad (4)$$

BIAS)
$$BIAS=\frac{1}{n}\sum_{i=1}^{n}(\hat{x_i}-x_i)=\overline{\hat{x_i}}-\overline{x_i} \quad (5)$$

RMSE(ROOT Mean Square Error)
$$RMSE=\sqrt{\frac{1}{n}\sum_{i=1}^{n}(\hat{x_i}-x_i)^2} \quad (6)$$

Here, $\hat{x_i}$는 CMDPS is calculated RI, x_i is AWS rainfall and SSM/I RI, n is number of data with temporal and spatial coincidence, and ¯ means average value. Correlation coefficient is used to find the corelation between CMDPS RI and the observed values. Bias and RMSE are used to evaluate the deviation of calculated RI and observed value.

B. Categorical accuracy test

Categorical accuracy is an important index to evaluate rainfall/non-rainfall area and RI accuracy of calculated result, in which PC(Portion Correct), POD(Probability of Detection) and HSS(Heidke Skill Score) are used. Binary category contingency table of RI and observed value to evaluate the presence of rainfall are seen in Table 2, and the accuracy is calculated in equation (7)~(10).

Table 2. Binary category contingency table for validation of CMDPS precipitation intensity.

		Observed		Estimated distribution
		Yes(≥0.5)	No(<0.5)	
Estimated	Yes(≥0.5)	a	b	a+b
	No(0.5<)	c	d	c+d
Observed distribution		a+c	b+d	

Portion Correct (PC) $$PC \quad \frac{a+d}{N} \tag{7}$$

Probability of Detection (POD , Hit Rate) $$POD = \frac{a}{a+c} \tag{8}$$

Heidke Skill Score (HSS) $$HSS = \frac{PC-E}{1-E} \tag{9}$$

$$E = \frac{(a+b)\times(a+c)+(c+d)\times(b+d)}{N} \tag{10}$$

PC(Portion Correct) is the ratio of same rainfall and non-rainfall data between calculated values and observed values and POD(Probability of Detection) is the accuracy of rainfall detection of calculated RI against the observed value. HSS(Heidke Skill Score) is used to evaluate the difference between accurate RI data and accidentally matched data from observed data. It is included in normalized accuracy calculation method. Multiple categorical accuracy evaluation can be made by categorizing RI into some forms or intensities. It is categorized into 3 steps of RI; mild (0.5~3mm/hr), intermediate (3~10 mm/hr) and strong (10 mm/hr~), and the multiple category contingency table (3×3) is shown in Table 3, and the accuracy calculation is like (11)~(14).

Table 3. Multiple Category contingency table for validation of CMDPS precipitation intensity.

		Observed			Estimated distribution
		0.5≤ RI <3.0	3.0≤ RI <10.0	10.0≤ RI	
Estimated	0.5≤ RI <3.0	A_{11}	A_{12}	A_{13}	R_1
	3.0≤ RI <10.0	A_{21}	A_{22}	A_{23}	R_2
	10.0≤ RI	A_{31}	A_{32}	A_{33}	R_3
Observed distribution		C_1	C_2	C_3	N

Portion Correct (PC)

$$C \frac{1}{N} \sum_{=1}^{3} A_{ii} \tag{11}$$

Heidke Skill Score (HSS)

$$HSS = \frac{NC - E}{N - E} \tag{12}$$

$$NC = \sum_{i=1}^{3} A_{ii} \tag{13}$$

$$E = \sum_{i=1}^{3} \frac{C_i R_i}{N} \tag{14}$$

4. Interpretation of Calculation Result

Calculation result is classified into final result and intermediate result. The final result is stored in HDF5 form as RI and quality information for whole area of data according to COMS observation mode. LUT, an intermediate result, and temporal and spatial coincidence data stored in ASCII format for Eastern Asian region and created during evaluation process and evaluation result are stored in binary format. Final results, RI and quality information result at 1933UTC July 23 2008 in Eastern Asian area are shown in Figure 14.

(a) Rainfall intensity (b) Quality flag

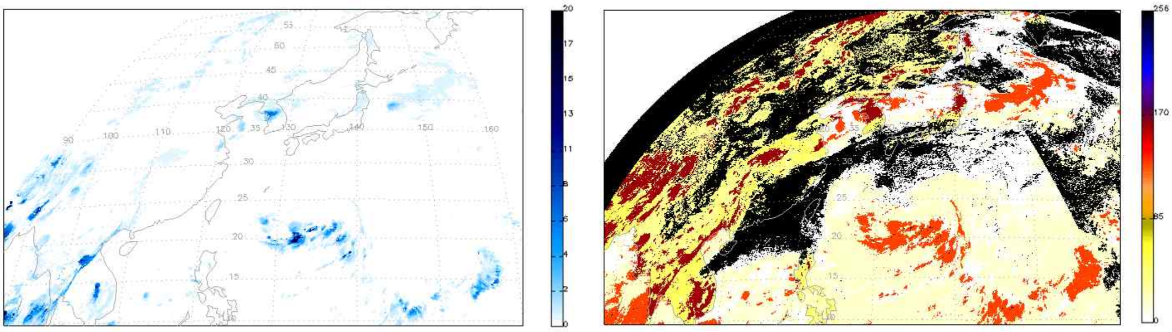

Figure 14. CMDPS rainfall intensity and Quality flag at 1933UTC July 23 2008.

RI is distributed from 0 to 20 mm/hr and darker blue means higher RI. As for quality flag, information on the calculation result for each pixel is obtained and it is interpreted using Table 1. Black area means an area in which RI is not calculated, referring the value of 256.

RI can quality flag are carried out when COMS observation data is present. RI calculation result is calculated and evaluated after coinciding with AWS observation data in Korean peninsular and with SSM/I RI data in Eastern Asian region. Figure 15 shows the point coincidence of RI calculation result, AWS observation data and SSM/I rainfall data at 1933UTC July 23 2008.

(a) Validation dataset between CMDPS RI and AWS RI

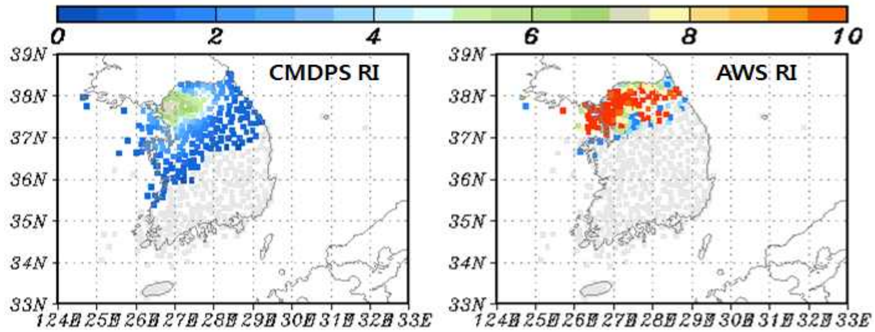

(b) Validation dataset between CMDPS RI and SSM/I RI

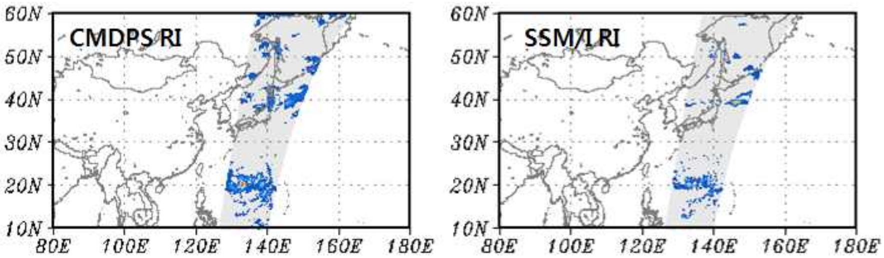

Figure 15. Validation dataset between CMDPS RI and AWS(a) and SSM/I(b) rainfall at 1933UTC July 23 2008.

In Figure 15, blue and red areas are where AWS and SSM/I pixels had temporal and spatial coincidence, and grey area does not have rainfall. In this figure, rainfall area calculated by CMDPS is distributed wider than SSM/I observation data, and RI is lower than AWS observation value (because the maximum rainfall is limited to 35 mm/hr). In this figure, the data pair of AWS and SSM/I resolution is evaluated according to the method mentioned in 3.4 and the result is shown in Table 4.

Table 4. The validation result between CMDPS RI and AWS and SSM/I rainfall at 1933UTC July 23 2008.

Validation (data #)	Scalar			Binary categorical			Multi categorical	
	R	BIAS	RMSE	POD	PC	HSS	PC	HSS
AWS(582)	0.77	-4.24	11.23	0.92	0.80	0.62	0.24	0.03
SSM/I(13595)	0.54	0.07	0.62	0.70	0.93	0.40	0.69	0.21

Out of AWS and SSM/I data, the number of data used in evaluation is 582 points in AWS and 13595 pixels of SSM/I. In the evaluation result using RI of SSM/I, RMSE is low despite the lower correlation coefficient than AWS rainfall. It is analyzed to be caused because SSM/I data was used to calculate RI of CMDPS. Because SSM/I RI data was used to calculate LUT, a negative bias occurs for AWS rainfall and RMSE was high. This causes relatively low PC in dual category or muti-category evaluation. Therefore, to evaluate RI calculation result with ground observed rainfall, it is analyzed that a precise understanding and analysis on CMDPS RI calculation range and microwave data are required first.

5. Problems and Areas of Improvement

Since rainfall distribution characteristics are not clearly distinguished in the limited channel data of COMS, the accuracy of RI calculation result by COMS data is limited. Therefore, to enhance the accuracy of RI by COMS channel data, cloud type can be limited by time and space or RI can be calculated directly using microwave channel, in the long term.

In this study, even though ground AWS data is used to evaluate RI calculation result, AWS data is a temporal accumulated data, while satellite observation data is temporary observation data. These two materials does not match in time. Therefore, to make an accurate verification and evaluation of RI result calculated by COMS data, dense rainfall observation data (AWS data) and radar data in specific area are required and the use is recommended. For the accuracy of calculated RI, temporal and spatial-statistic evaluation is considered to be more important than the evaluation of each pixel. It will contribute to enhancement of COMS RI calculation accuracy when various microwave data (SSMIS, AMSU, AMSR/E, TRMM TMI)are used as well as current SSM/I (F15) data.

6. References

Adler, R. F., and A. J. Negri, 1988 : A satellite infrared technique to estimate tropical convective and stratiform rainfall. J. Appl. Meteor., 27, 30-51.

Arkin, P. A., 1979 : The relationship between fractional coverage of high cloud and rainfall accumulations during GATE over the B-scale array. Mon. Wea. Rev., 107, 1382-1387.

Arkin, P. A., and B. M. Meisner, 1987 : The Relationship between Large-Scale Convective rainfall and Cold Cloud over the Western Hemisphere during 1982-84.

Mon. Wea. Rev., 115, 51-74.

Atlas, D., D. Rosenfeld, and D. B. Wolff, 1990 : Climatologically tuned reflectivity-rainrate relations and links to area-time integrals. J. Appl. Meteor., 29, 1120-1135.

Ba, M., and A. Gruber, 2001 : GOES Multispectral rainfall Algorithm(GMSRA). J. Appl. Meteor.,29,1120-1135.

Crosson, W. L., C. E. Duchon, R. Raghavan, and S. J. Goodman, 1996 : Assessment of rainfall estimates using a standard Z-R relationship and the probability matching method applied to composite radar data in Central Florida. J. Appl. Meteor., 35, 1203-1219.

Delgado, G., Luiz A. T. Machado, Carlos F. Angelis, Marcus J. Bottino, Á. Redaño, J. Lorente, L. Gimeno, and R. Nieto, 2008 : Basis for a rainfall Estimation Technique Using IR–VIS Cloud Classification and Parameters over the Life Cycle of Mesoscale Convective Systems. J. of Appl. Meteol and Clim., 47, 1500-1517.

Inoue,T. and S. A. Ackerman, 2002 : Radiative Effects of Various Cloud Types as Classified by the Split Window Technique over the Eastern Sub-tropical Pacific Derived from Collocated ERBE and AVHRR Data., J. of Meteorological Society of Japan, 80,1382-1394.

Inoue, T., 1987 : A cloud type classification with NOAA-7 split-window measurements. J. Geophys. Res., 92, 3991-4000

Joyce, R. J., J. E. Janowiak, P. A. Arkin, and P. Xie, 2004 : CMORPH: A Method that Produces Global rainfall Estimates from Passive Microwave and Infrared Data at High Spatial and Temporal Resolution, J. of Hydrometeor., 5(3), 487–503.

Kuligowski, R. J., 2002 : A self-calibrating GOES rainfall algorithm for short-term rainfall estimates. J. Hydrometeor.,3, 112-130.

Kummerow C., Y. Hongb, W. S. Olsonc, S. Yangc, R. F. Adlerd, J. McCollume, R. Ferraroe, G. Pettyf, D-B. Shina, and T. T. Wilheitg, 2001 : The evolution of the Goddard profiling algorithm (GPROF) for rainfall estimation from passive microwave sensors. J. Appl. Meteor., 40, 1801–1820.

Kurino, T., 1997 : A satellite infrared technique for estimating "deep/shallow" convective and stratiform precipitation. Adv. Space Res., 19. 511-514.

Lavizzani, V., 1999. Convective rain from a satellite prospective: Achievements and challenges. SAF Training Workshop-Nowcasting and Very Short Forecasting, Madrid, 9-11 Dec., EUMESAT, EUM P 25, 75-84.

Negri, A. J., R. F. Adler, and P. J. Wetzel, 1984 : Rain estimation from satellites: an examination of the Griffith-Woodley technique, J. Climate Appl. Meteor., 26, 1565-1576.

Scofield, R. A. and R. J. Kuligowski, 2003 : Status and Outlook of Operational Satellite Precipitation Algorithms for Extreme-Precipitation Events., Weather and Forecasting,18,1037–1051.

Sorooshian, S., K.-L. Hsu, X. Gao, H. V. Gupta, B. Imam, and D. Braithwaite, 2000 : An evaluation of PERSIANN system satellite-based estimates of tropical rainfall. Bull. Amer. Meteor. Soc., 81, 2035-2046.

Spencer R. W., H. M. Goodman, and R. E. Hood, 1989 : Precipitation retrieval over land and ocean with the SSM/I: Identification and characteristics of the scattering signal. J. Atmos. Oceanic Technol., 6, 254–273.

Turk, F. J., E. E. Ebert, H.-J. Oh, B.-J. Sohn, V. Levizzani, E. A. Smith and R. R. Ferraro, 2003 : Validation of an operational global precipitation analysis at short time scales. Prepr. 12th Conf. on Satellite Meteor. and Oceanography, Long Beach, CA, 9-13 Feb., paper 1.2, 21.

Vincente, G. A., R. A. Scofield, and W. P. Menzel, 1998 : The operational GOES infrared rainfall estimation technique. Bull. Amer. Meteor. Soc., 79,1883-1898.

Vincente, G. A., J. C. Davenport, and R. A. Scofield, 2002 : The role of orographic and parallax on real time high resolution satellite rain rate distribution. Intl. J. Remote Sens., 23, 221-230.

Weng, F., L. Zhao, G. Poe, R. R. Ferraro, X. Li, and N. C. Grody, 2003 : Advanced Microwave Sounding Unit (AMSU) cloud and precipitation algorithms. Radio Sci., 38(4), 8068, doi:10.1029/2002RS002679.

Wentz, Frank J. and Roy W. Spencer, 1998 : SSM/I Rain Retrievals within a UnifiedOcean Algorithm, J. of Atmos. Sci., 55, 1613-1627.

Zhang, M., and R. A. Scofield, 1994 : Artificial neural network techniques for estimating convective rainfall and recognizing cloud mergers from satellite data. Int. J. Remote Sens., 15, 3241-3261.